

EMRIs and the relativistic loss-cone: The curious case of the fortunate coincidence

Tal Alexander

Dept. of Particle Physics and Astrophysics, Weizmann Institute of Science, Rehovot, Israel

E-mail: tal.alexander@weizmann.ac.il

Abstract. Extreme mass ratio inspiral (EMRI) events are vulnerable to perturbations by the stellar background, which can abort them prematurely by deflecting EMRI orbits to plunging ones that fall directly into the massive black hole (MBH), or to less eccentric ones that no longer interact strongly with the MBH. A coincidental hierarchy between the collective resonant Newtonian torques due to the stellar background, and the relative magnitudes of the leading-order post-Newtonian precessional and radiative terms of the general relativistic 2-body problem, allows EMRIs to decouple from the background and produce semi-periodic gravitational wave signals. I review the recent theoretical developments [1] that confirm this conjectured fortunate coincidence [2], and briefly discuss the implications for EMRI rates, and show how these dynamical effects can be probed locally by stars near the Galactic MBH.

1. Introduction

Extreme mass ratio inspiral (EMRI) gravitational wave (GW) emission events, where a stellar mass black hole (BH) of mass M_\star gradually inspirals into a massive BH (MBH) of mass M_\bullet , are one of the main classes of anticipated extra-galactic low-frequency GW sources. Since $Q = M_\bullet/M_\star \gg 1$, such BHs probe spacetime near the MBH almost as test particles, and thereby offer an opportunity to test general relativity (GR) under theoretically favorable conditions.

However, the inspiral process is not simply a 2-body problem in the strong gravity regime. The MBH is surrounded by $\mathcal{O}(Q)$ background stars inside its radius of dynamical influence $r_h \sim GM_\bullet/\sigma^2$, where σ^2 is the stellar velocity dispersion in the host galaxy's spheroidal. The complex dynamics of the stellar cluster around the MBH, that supplies stars that fall into the MBH, whether directly on plunging orbits, or indirectly on inspiraling ones, also interferes with the idealized 2-body motion of the light BH relative to the MBH, and can even suppress inspiral altogether.

I show here that EMRIs are in fact possible by virtue of a three-way fortunate coincidence between the magnitude and timescale of collective Newtonian effects due to the background stars, which give rise to strong resonant gravitational torques, and those of the leading-order precessional and radiative post-Newtonian (PN) terms of GR [2]. This curious coincidence raises several questions: How fine-tuned is it? Is this a specific feature of Einstein's GR, or is it generic to a larger class of theories of strong gravity? Do still-viable alternatives to GR predict substantially different plunge / inspiral branching ratios? Could the very detection of an EMRI in the future rule out some of them? These questions remain open at this time.

Another consequence of the fortunate coincidence is that rapid relaxation by resonant torques in the symmetric potential near a MBH [3], which can dominate slow 2-body relaxation in some

regions of phase space [4], is ultimately not very important in determining the steady-state loss-rates (e.g. by tidal disruption or GW inspiral). By a coincidence that can only be understood in the context of the relativistic loss-cone dynamics, early naive estimates that included only a partial treatment of Newtonian dynamics (2-body relaxation, but not resonant torques) and of GR dynamics (GW dissipation but not in-plane Schwarzschild precession), yielded correct order of magnitude loss-rates estimates [5].

Here I briefly review the recent developments in the understanding and modeling of the relativistic loss-cone that lead to these insights, focusing on the relevance for EMRI rates, and on the prospects of probing these dynamical mechanisms locally, near the Milky Way's MBH Sgr A*.

1.1. The loss-cone problem

Orbits whose periastron lies inside the tidal radius $r_t = R_\star Q^{1/3}$ (where R_\star is the stellar radius) or inside the last stable orbit $r_\bullet \simeq 8r_g$ (where $r_g = GM_\bullet/c^2$) are classified as plunges. In terms of the normalized angular momentum $j = J/\sqrt{GM_\bullet a} = 1 - e^2$ (where a is the orbital semimajor axis (sma) and e the eccentricity), the corresponding plunge conditions are $j < j_{lc} = j_t \simeq \sqrt{2r_t/a}$ or $j < j_{lc} = j_\bullet = \sqrt{16r_g/a}$. Since the set of velocity vectors that take a star from position \mathbf{r} to the MBH span a cone, the set of such orbits are called the loss-cone. Stars in the loss-cone are destroyed in less than an orbital period. In steady state, new stars have to be deflected to loss-cone orbits, and therefore the loss-cone problem is the problem of how a stellar system around a MBH randomizes. In a spherical potential, where the angular momentum of individual orbits is conserved in collisionless motion, randomization is achieved by dynamical relaxation.

1.2. Loss-cone replenishment by dynamical relaxation

The classical treatments of the loss-cone problem considered only slow 2-body relaxation (denoted here also non-resonant relaxation, NR), which is inherent to any system composed of discrete interacting particles [6, 7, 8, 9]. A relaxed stellar system around a MBH settles into a high density powerlaw stellar cusp, $n_\star \propto r^{-\alpha}$. For a single mass population, which we consider here for simplicity, $\alpha = 7/4$ [7]. Near a MBH, the 2-body relaxation timescale can be expressed as $T_{NR}(a) \sim Q^2 P(a)/N_\star(a) \log Q$, where P is the orbital period, $N_\star(a) \sim Q(a/r_h)^{3-\alpha}$ is the number of stars with sma $< a$, and $\log Q$ is the Coulomb factor [1].

Generally, the 2-body relaxation timescale for changing the angular momentum J by order of itself, T_J , is related to the relaxation timescale for changing the energy E by order of itself, T_E , by $T_J \sim j^2 T_E$ [5]. It is therefore faster to reach the MBH by relaxation of angular momentum than by relaxation of energy (equivalently, relaxation of the sma, since $E = GM_\bullet/2a$, using the stellar dynamical convention $E > 0$ for bound orbits).

In the presence of orbital dissipation (e.g. by the emission of GWs, by tidal deformations of the star close to the MBH, or by hydrodynamical interactions with a massive accretion disk), the star can also fall into the MBH by gradually losing orbital energy. Such orbits are classified as inspirals. Because inspiral, unlike a plunge, requires many consecutive periastron passages, such orbits are much more susceptible to perturbations by the stellar background, unless the inspiral already starts from a tight orbit around the MBH. phase space is therefore separated into two regimes (Fig. 1). Close to the MBH, below some critical sma a_{GW} (here we consider only dissipation by GWs), stars are statistically much more likely to reach the MBH by inspiral, whereas above a_{GW} and up to $a \sim r_h$, plunges are much more likely. The transition is sharp [10]. The plunge rate is $R_p \sim N_\star(r_h)/\log(1/j_{lc})T_E(r_h)$, while the inspiral rate is $R_i \sim N_\star(a_{GW})/\log(1/j_{lc})T_E(a_{GW})$ [11]. Since the relaxation timescale is typically not a strong function of distance, the branching ratio $R_i/R_p \sim N_\star(a_{GW})/N_\star(r_h)$ reflects the relative number of sources in the small phase space volume interior to a_{GW} and the much larger one

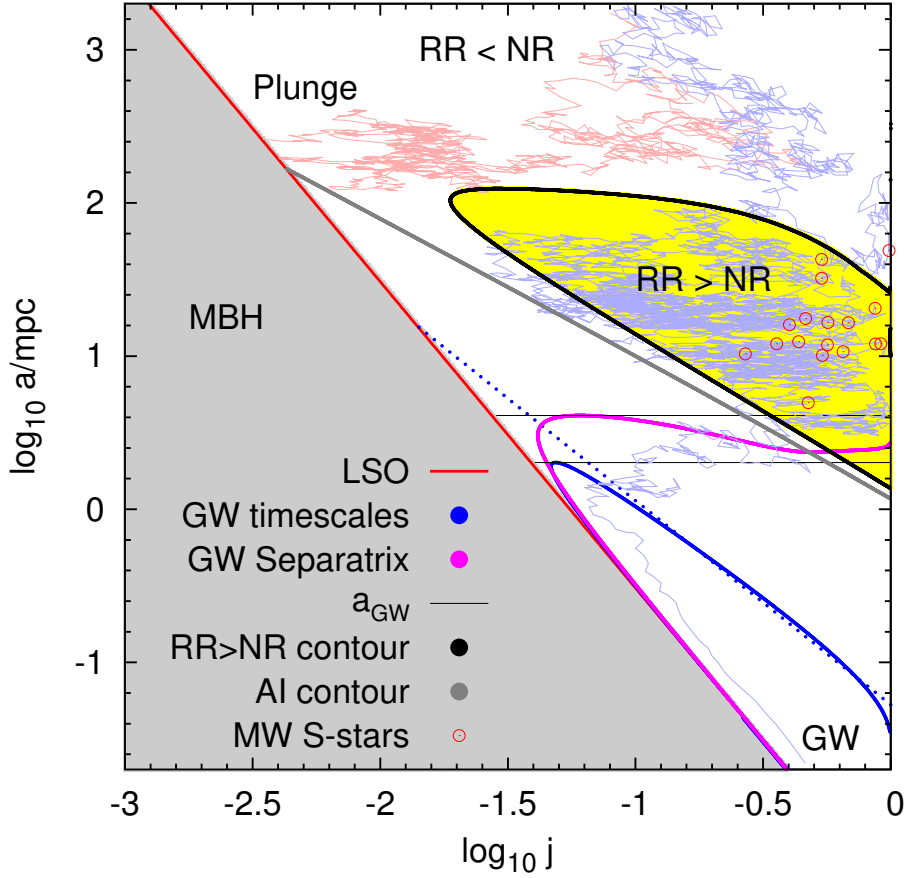


Figure 1. A schematic of the relativistic loss cone in $(\log j, \log a)$ phase space for a simplified model of the Milky Way (MW) nucleus with a $M_{\bullet} = 4 \times 10^6 M_{\odot}$ MBH surrounded by a relaxed cluster of $10 M_{\odot}$ stellar BHs [4]. The gray region to the left, below the last stable orbit (LSO) line demarcates the region of unstable orbits. Stars diffuse from the Galaxy beyond the radius of influence at the top ($a \gtrsim 2$ pc) and either wander back to the Galaxy, plunge directly into the MBH across the LSO (the light red track is a Monte Carlo generated track of a plunge event), or diffuse deeper into the cusp until they cross the GW separatrix (magenta curve), where the streamlines of the probability density flux turn over to the region where GW dissipation is faster than 2-body relaxation (blue curve). The critical sma a_{GW} (black horizontal lines, at two possible extreme values) approximately separates phase space into a region $a > a_{GW}$ where the stellar BHs plunge directly into the MBH, and a small phase space volume at $a < a_{GW}$ where the BHs inspiral into the MBH. RR is quenched by fast precession below the AI line (gray line), and the trajectories appear to “bounce” against it due to the strong gradient in the effective RR diffusion coefficient (Fig. 3). RR is faster than NR only in a restricted region of phase space (yellow region), where motion along the j -direction is much faster than in the a -direction. Since the RR-dominated region is well-separated from the plunge and EMRI loss-lines, RR has only a small effect on the steady state loss-rates (cf Fig. 5). However, it has a strong effect on the orbits of the observed S-stars, which happen to lie in this phase space region (Sec. 3.2).

inside r_h . For that reason inspiral events are generally much rarer than plunges, $R_i \sim \mathcal{O}(0.01)R_p$ [12].

Resonant relaxation [3, 2] is a form of rapid relaxation of angular momentum that occurs in potentials with a high degree of symmetry, which restrict orbital evolution (e.g. fixed

Keplerian ellipses in the Newtonian potential of a point mass; fixed orbital planes in a spherical potential). The approximately spherical, point mass-dominated potential around a MBH is such a potential. Far enough from the MBH where GR effects are small, but close enough to it, where deviations from Keplerian motion due to the distributed stellar mass are also small, the orbits are nearly-Keplerian ellipses (for Sgr A^* this distance scale corresponds to 0.01 – 0.1 pc [2]), which persist over a long coherence time $T_c \gg P$. On that timescale, the N_* background stars can be viewed as fixed elliptical mass “wires”. A test star orbiting the MBH with sma a in the potential generated by the background, will conserve its energy (since the wires are stationary), but will be subject to a non-zero residual force of order $F_N \sim \mathcal{O}(\sqrt{N_*(a)}GM_*/a^2)$, which translates to a coherent torque $\tau_N \sim \mathcal{O}(\sqrt{N_*(a)}GM_*/a)$. This torque persists in magnitude and direction over time T_c , until the small deviations from perfect symmetry accumulate and randomize the background. The change in angular momentum over the coherence time, $(\Delta J)_c = \tau_N T_c$ then becomes the mean free path in J -space for a random walk on timescale $t \gg T_c$: $\Delta J = (\Delta J)_c \sqrt{t/T_c} \rightarrow \Delta j = \sqrt{t/T_{RR}}$, where the RR relaxation timescale is $T_{RR} \sim [Q^2/N_*(a)]P^2(a)/T_c(a)$.

The ratio between the RR and NR relaxation times, $T_{RR}/T_{NR} \sim \log Q(P/T_c)$ reflects the fact that NR occurs by point-point interactions, and is boosted by the closest strong interactions, whereas RR occurs by orbit-orbit interactions, which as extended objects cannot approach each other arbitrarily close, but are boosted by the long coherence time. The relevance of RR to the loss-cone problem is due to the fact that near a MBH, it is possible to have $T_{RR}/T_{NR} \ll 1$. This implies very rapid angular momentum evolution, and specifically $j \rightarrow 0$, which allows strong interactions with the MBH.

1.3. The fortunate coincidence

The strong RR torques inside $a_{GW} \ll a \ll r_h$, if unquenched, would drive all stars directly into the MBH on plunge orbits and the EMRI rate would drop to zero. Hopman & Alexander conjectured in 2006 [2] that EMRIs will in fact occur because the PN1 $\mathcal{O}(\beta^2 j^{-2})$ GR precession becomes significant enough to quench RR before the PN2.5 $\mathcal{O}(\beta^5 j^{-7} Q^{-1})$ GW dissipation rate becomes fast (here $\beta = v/c$). This was later confirmed in N -body simulations [13, 14] (but see Sec. 1.4), and was also demonstrated by Monte Carlo (MC) simulations of diffusion in the relativistic loss-cone [4] (Sec. 2). Fig. (2) shows that GR Schwarzschild precession has a drastic effect on the steady state phase space densities and rates. EMRIs exist because of a fortunate coincidence in the ranking and phase space dependence of the magnitude of the RR torques, which are a collective Newtonian effect, and the magnitudes of GR’s leading order precessional and radiative terms, which are post-Newtonian 2-body effects.

1.4. An unexpected result

The first direct N -body simulation with self-consistent post-Newtonian terms (up to PN2.5, the lowest-order radiative term) [13] yielded an unanticipated result. Not only did GR precession quench RR on eccentric orbits, as conjectured, but in fact it appeared that a barrier in phase space, the “Schwarzschild Barrier” (SB), prevented stars from reaching either the LSO or the GW line (cf Fig. 3). The phase space trajectories of stars seemed to linger near the SB for about a coherence time, while their orbital parameters oscillated at at the Schwarzschild precession frequency, before being reflected back to less eccentric orbits. Larger-scale N -body simulations subsequently confirmed the quenching of RR by GR precession near the SB [14]. Although an early analysis indicated that the SB is related to precession under the influence of a randomly changing uniform force [15, 13], the nature and implications of the SB phenomenon remained controversial.

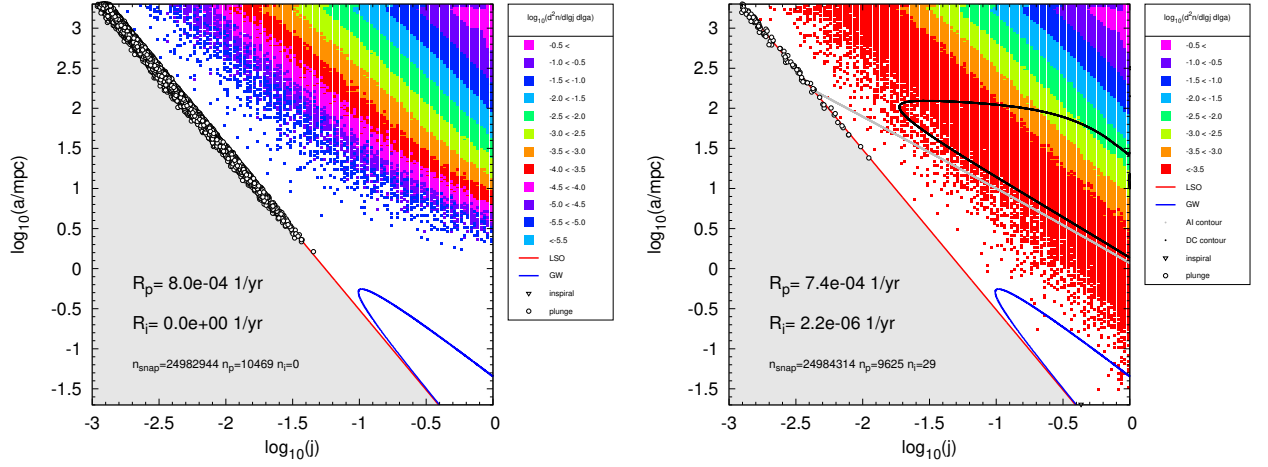


Figure 2. The steady state density in phase space as derived from Monte Carlo simulations of loss-cone dynamics for a simplified model of the Milky Way nucleus surrounded by stellar BHs (see Fig. 1), taking into account the dynamical effects of NR, RR (with the η -formalism) and GR (leading order precession and GW) [4]. The plunge and inspiral rates (R_p , R_i) are quoted on the plot. The end points of a sample of the trajectories are marked by small black circles. Top: GR Schwarzschild precession turned off. In the absence of quenching, the strong RR torques sweep all BHs to plunge orbits well above the GW loss-line, and the EMRI rate drops to zero. Bottom: All dynamical effects are included. The system reaches a steady state that is very close to thermal, with a finite inspiral rate $R_i \sim \mathcal{O}(10^{-6} \text{ yr}^{-1}) < 0.01 R_p$.

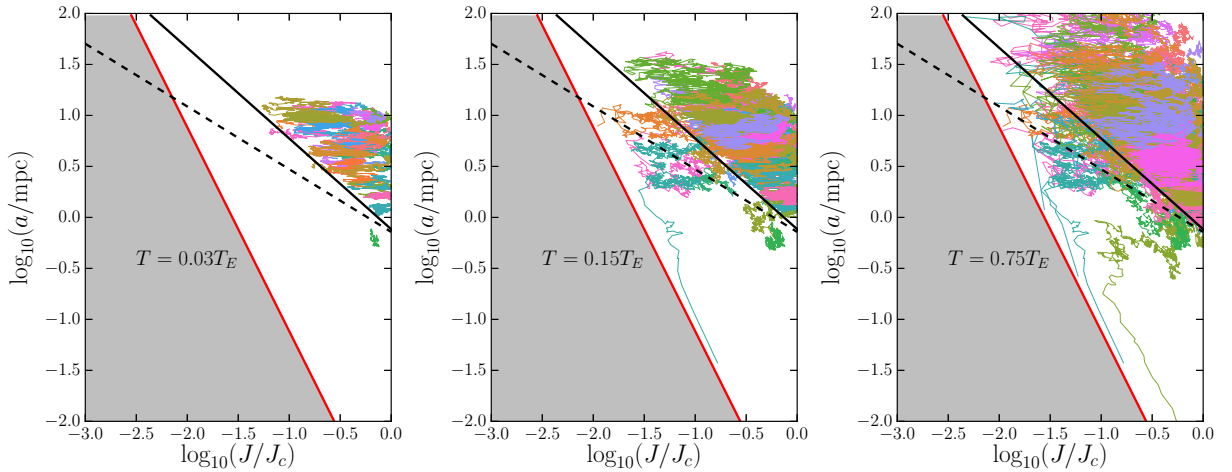


Figure 3. The nature of the SB / AI line. A time sequence (left to right) of three snapshots showing the phase space trajectories of 50 stars of mass $50 M_\odot$ each, in a relaxed cusp ($\alpha = 7/4$) around a MBH of $10^6 M_\odot$ [4]. The AI locus is denoted by a solid black line (the dashed line is the mis-identified locus of the SB [13]). At times much shorter than the NR energy relaxation timescale T_E , evolution by rapid RR dominates, but can occur only above the AI line. As time progresses, NR, which is unaffected by AI, populates phase space beyond the AI line, and ultimately establishes the maximal entropy (thermal) equilibrium on timescales $\gtrsim \mathcal{O}(T_E)$, irrespective of AI.

2. The η -formalism for relativistic loss-cone dynamics

Relativistic loss-cone dynamics, and in particular the interplay between secular precession, the coherent RR torques, and uncorrelated NR, lie in the difficult-to-treat interface between deterministic Hamiltonian dynamics and stochastic kinetic theory. The η -formalism [1] provides a formal framework for treating this regime by stochastic equations of motion (EOMs) that describe the dynamics, by identifying the relevant features of the stochastic effects of the stellar background on the test star, and importantly, by enabling the description of RR dynamics by effective diffusion coefficients, in spite of the fact that the long RR coherence time makes it a manifestly non-Markovian process that cannot be described, as is, by diffusion.

The key idea of the η -formalism is to describe the effect of the background stars in terms of a time-correlated noise model. A perturbative expansion of the phase-averaged post-Newtonian Hamiltonian to leading order shows that the symmetries of the noise are those of a vector in angular momentum space, $\boldsymbol{\eta}(t)$ ¹. The dynamics of the system are then primarily determined by the temporal smoothness (differentiability) of the noise, and by its coherence time T_c . Neither of these properties are known at present from first principles or from N -body simulations. However, since the collective effect of the background is due to the superposition of many smooth orbital motions, it is likely that the noise is smooth (infinitely differentiable). A smooth noise must have an maximal frequency $\nu_{\max} \propto 1/T_c$, beyond which its power decays rapidly.

When the GR precession frequency, $\nu_{GR}(a, j) = 3(c/r_g)(r_g/a)^{5/2}j^{-2}$ (where $r_g = GM_{\bullet}/c^2$) is higher than $1/T_c$ (i.e. when the precession period is much shorter than the coherence time), the residual RR force is effectively constant over a precession period, so the RR torque on the precessing eccentric star is reversed every half cycle. Therefore, the net change in j per period is canceled to high precision—the rapidly precessing eccentric orbit is decoupled from the slowly varying stellar background by adiabatic invariance (AI). This happens along the phase space locus

$$j_{AI}(a) = \sqrt{T_c(a)\nu_{GR}(a, j = 1)/2\pi}. \quad (1)$$

The stochastic EOMs allow to evolve in time the phase space trajectory of a test star, for a given random realization of the background noise. The fact that the noise is approximately a function of time only, makes it possible to formally derive an effective diffusion coefficient for RR, $D_{jj}(a, j)$, which is proportional to the power of the noise at $\nu_{GR}(a, j)$, and is therefore strongly suppressed below the AI locus. This then makes it possible to directly evolve the stellar distribution function by the Fokker-Planck (FP) equation. The great practical advantage of an effective RR diffusion formulation is that it is then possible to model the dynamics of the loss-cone in the realistic $N_{\star} \rightarrow \infty$ limit by an MC procedure that solves the FP equation statistically, and where it is easy to include also NR, the secular precessions due to GR and the enclosed stellar mass, and dissipation by GW (and by tidal heating, when relevant). The MC results are able to reproduce the SB phenomenology observed in the N -body simulations, as well as the plunge and inspiral rates [4]. Fig. (3) shows how the AI/SB phenomenon is reproduced by effective RR diffusion, and also how on long timescales the NR dominates the dynamics, and the system asymptotes to the maximal entropy solution, as it must irrespective of the randomization mechanism².

2.1. How fine-tuned is the fortunate coincidence?

A simple estimate for the degree of fine-tuning needed for the fortunate coincidence can be derived by artificially varying the Schwarzschild precession frequency by a constant factor,

¹ The noise can be approximated as independent of j because the mean free path in j due to RR is small.

² The fact the the system is not closed, and there is a small stellar flux into the less cone, makes possible small deviations from the maximal entropy solution.

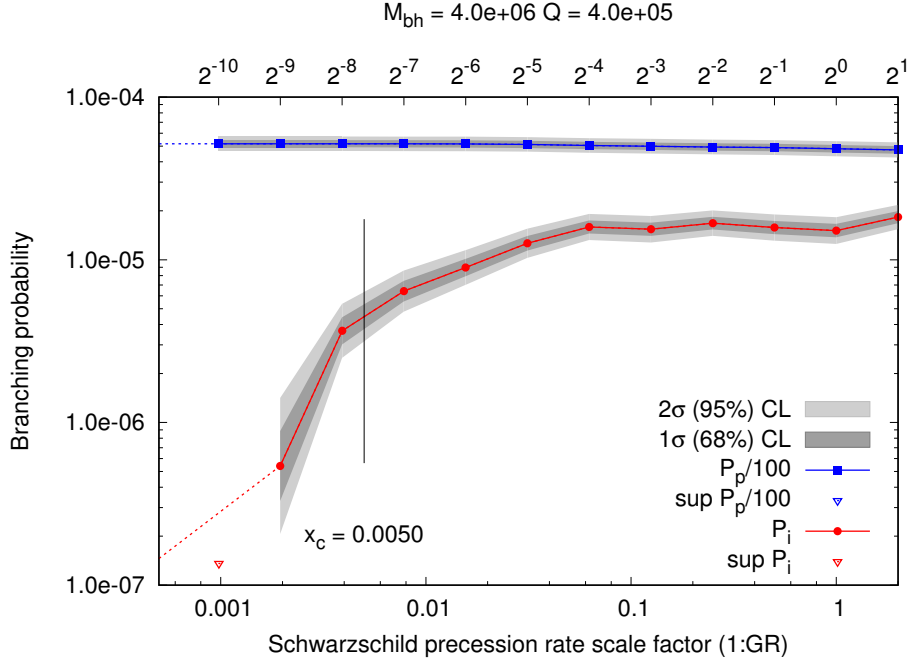


Figure 4. The run of the plunge and inspiral branching probabilities with the precession frequency scaling factor x ($x = 1$ corresponds to GR) for a simplified Milky Way model with $M_{\bullet} = 4 \times 10^6 M_{\odot}$ and $M_{\star} = 10 M_{\odot}$. The blue line is the plunge probability (divided by 100 to allow a more compact plot). A dotted blue line connects it to $P_p(x = 0)$. The red line is the inspiral (EMRI) probability. A dotted red line connects it to the result $P_i(x = 0) = 0$. The gray areas around the lines are the 1σ and 2σ regions, respectively. The vertical line is the theoretically derived critical value for x (see text).

$\nu_x = x\nu_{GR}$ ($x \geq 0$), and testing how this affects the branching ratio between plunges and inspirals. In terms of the phase space shown in Fig. (1), a scaling factor $x < 1$ shifts the AI line parallel to itself downward, and extends the region where RR is effective. A simple criterion for predicting the effect of the scale factor is the position of the intersection point of the AI locus and the LSO line relative to the critical sma for EMRIs, a_{GW} (Figure 1). EMRIs are no longer possible when RR is effective at all values of $j_{lc} \leq j \leq 1$ down to the critical sma for EMRIs, a_{GW} , since then all stars are swept into the MBH on plunging trajectories before they can diffuse below a_{GW} . This occurs when the AI locus $j_0(a; x) = \sqrt{T_c(a)\nu_x(a, j = 1)/2\pi}$, crosses the plunge loss cone $j_{\bullet}(a)$ below $a_{GW} \simeq 0.03(\log Q)^{-4/5}r_h$ [4], where a relaxed cusp with $\alpha = 7/4$ is assumed, and where the numeric prefactor depends on the approximation of the GW dissipation. The scaling of r_h with Q (assuming an M_{\bullet}/σ relation $M_{\bullet} \propto \sigma^4$ and fixed M_{\star}) is $r_h \propto Q^{1/2}$, and so $a_{GW} \propto (\log Q)^{-4/5}Q^{1/2}$. The condition $j_0(a_{GW}; x_c)/j_{lc}(a_{GW}) = 1$ then defines a critical value x_c such that for $x < x_c$, RR remains unquenched everywhere above a_{GW} . Fig. (4) shows the run of the branching ratio with x for the Milky Way model of Fig. (1). The ratio changes in favor of plunges (cf. Fig. 2) for $x < x_c \sim \mathcal{O}(5 \times 10^{-3})$. This suggests that EMRIs are robust in the context of Einstein’s GR.

3. Applications of the η -formalism

3.1. Cosmic loss-rates

MC simulations such as the one presented in Fig. (2) for $M_{\bullet} = 4 \times 10^6 M_{\odot}$ can be carried out for any value of M_{\bullet} once the properties of the galactic nucleus are related to the MBH mass via

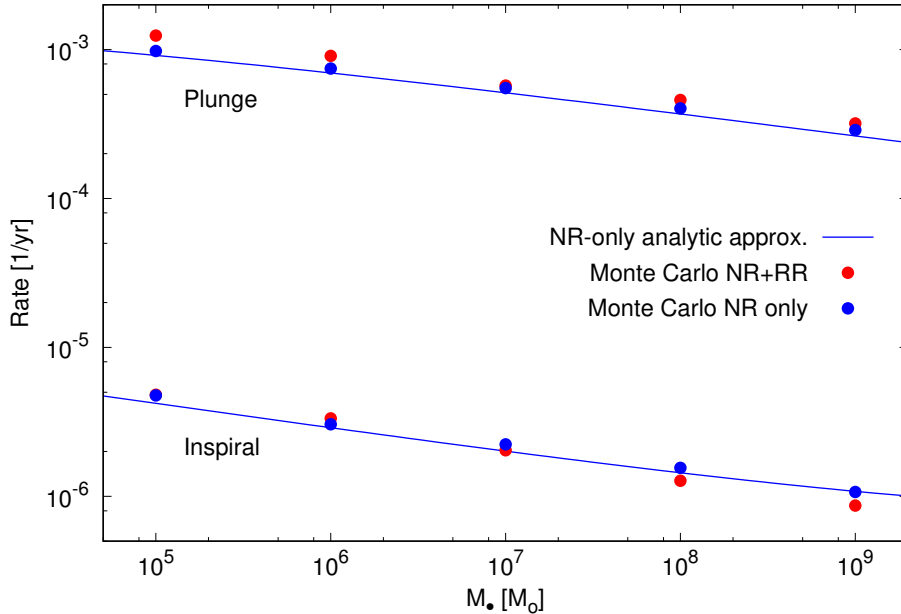


Figure 5. The plunge and inspiral rates, as function of the MBH mass M_\bullet , as derived from Monte Carlo simulations of the loss-cone in a sequence of simplified galactic nuclei models (adapted from [4]). The presence of RR makes only a small difference to the rates, since the loss lines (cf Figure 1) are well below the AI line (Eq. 1). The Inspiral rates are < 0.01 smaller than the plunge rate (Sec. 1.1), and both fall roughly as $M_\bullet^{-1/4}$ (for an M_\bullet/σ relation with $\beta = 4$).

the M_\bullet/σ relation. Fig. (5) Shows the run of the steady state plunge and EMRI inspiral rates as function of the MBH mass [4], and demonstrates the fact that RR plays only a small role in the rates, due to the very effective AI suppression of RR well away from the plunge and inspiral loss-lines (Fig. 1).

3.2. Loss-cone dynamics around the MBH of the Milky Way

One intriguing result that follows from the formal treatment of effective RR diffusion, and of the identification of the phase space region where RR dominates the dynamics, is that almost all the observed S-stars around Sgr A^* [16] (main sequence B stars, with masses $\sim 5 - 20 M_\odot$ and lifespans $\sim 10^7 - 10^8$ yr) are found inside the strong RR region (Fig. 6). This suggests that whatever the unknown formation (or capture, or migration) process that is responsible for the puzzling presence of young massive stars so deep in the potential of a MBH, it is likely that they have undergone strong post-formation j -evolution. Fig. (6) shows a preliminary attempt to discriminate between the two leading models for the origin of the S-stars: Capture by a 3-body tidal interaction of the MBH with an incoming massive stellar binary [17, 18] (tidal binary capture, or the Hills mechanism [19]), or migration from the observed stellar disk around Sgr A^* [20]. In addition, such models also probe the unobserved population of faint stars and remnants around the MBH, which are necessary for generating the RR torques, but whose presence is observationally controversial [21, 22, 23] (but see recent detection of a cusp of faint low mass stars in the Galactic Center [24, 25]). The MC experiments indicate that the likeliest scenario is that the S-stars were captured in tidal binary separation events, and their orbits subsequently evolved in the presence of high density “dark” stellar cusp.

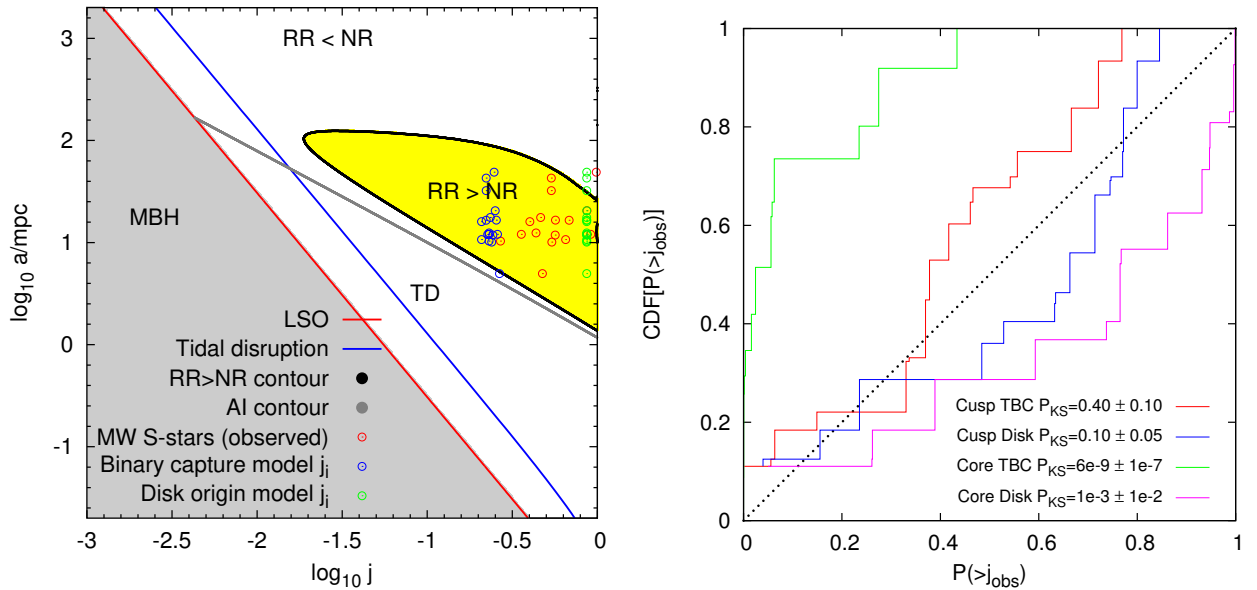


Figure 6. A joint test for the existence of a high density stellar cusp around Sgr A^* and for the origin of the S-stars that are observed to orbit the MBH in the central ~ 0.04 pc. Left: The S-stars [16] (red circles) lie in the phase space region where RR dominates the dynamics (the tidal disruption line for a typical S-star is shown in blue). If they originated from tidal binary captures (TBC, the Hills mechanism [19]), they start their existence near the MBH on highly eccentric orbits (blue circles), at an arbitrary phase of their lifespan. However, if the S-stars originated from the young ($\sim 6 \times 10^6$ yr [26]) stellar disk around observed around Sgr A^* , they are only as old as the disk, and are expected to originate on nearly circular orbits (green circles). Right: A comparison of the final cumulative j -distribution of the S-stars for the two formation scenario, as derived from MC simulations for two possible stellar distributions around the MBH: a dense relaxed cusp, and an out-of-equilibrium lower density stellar core. The best fit scenario (highest K-S probability with distribution closest to a straight line) is the tidal binary capture in a high density stellar cusp (Sabsovich, Alexander & Bar-Or, in prep.).

4. Summary

The complex dynamics that ultimately lead stars and compact remnants to fall into the MBH can be modeled by MC simulations that introduce RR by effective diffusion coefficients that are derived from the η -formalism. Phase space is clearly separated into a restricted region where RR dominates the dynamics, and a region where AI strongly suppresses RR due to fast precession. Elsewhere, RR exists, but NR is faster. Importantly, both the the loss-lines for plunges (LSO) and for GW EMRIs lie below the AI locus, and so RR has only a small effect on the loss-rates. This situation appears to be a fortunate coincidence for the prospects of detecting EMRIs. It is a result of a three-way competition between RR torques that tend to push stars to plunge orbits, GR Schwarzschild precession, which suppresses RR, and GR GW dissipation, which when fast enough, can be completed before the stellar background interferes. This coincidence appears robust in the context of Einstein's GR. It is however still unclear how general it is in the wider context of theories of strong gravity.

The dynamical processes that play part in EMRI dynamics can be probed by the puzzling S-stars observed near the MBH of the Galactic Center, which are at the RR-dominated region of the phase space around Sgr A^* .

Acknowledgments

This work was supported by the I-CORE Program of the Planning and Budgeting Committee and The Israel Science Foundation (grant No 1829/12).

References

- [1] Bar-Or B and Alexander T 2014 *Classical and Quantum Gravity* **31** 244003 (*Preprint* 1404.0351)
- [2] Hopman C and Alexander T 2006 *ApJ* **645** 1152–1163
- [3] Rauch K P and Tremaine S 1996 *New Astronomy* **1** 149–170
- [4] Bar-Or B and Alexander T 2016 *ApJ* **820** 129 (*Preprint* 1508.01390)
- [5] Alexander T 2017 *ArXiv e-prints* (*Preprint* 1701.04762)
- [6] Frank J and Rees M J 1976 *MNRAS* **176** 633–647
- [7] Bahcall J N and Wolf R A 1976 *ApJ* **209** 214–232
- [8] Shapiro S L and Marchant A B 1978 *ApJ* **225** 603–624
- [9] Bahcall J N and Wolf R A 1977 *ApJ* **216** 883–907
- [10] Hopman C and Alexander T 2005 *ApJ* **629** 362–372
- [11] Lightman A P and Shapiro S L 1977 *ApJ* **211** 244–262
- [12] Alexander T and Hopman C 2003 *ApJ* **590** L29–L32
- [13] Merritt D, Alexander T, Mikkola S and Will C M 2011 *Phys. Rev. D* **84** 044024 (*Preprint* 1102.3180)
- [14] Brem P, Amaro-Seoane P and Sopena C F 2014 *MNRAS* **437** 1259–1267 (*Preprint* 1211.5601)
- [15] Alexander T 2010 *GW and EM signatures of MBH binaries and EMRIs, APC, Paris* ed Amaro-Seoane P and Porter E online http://www.aei.mpg.de/~pau/conf_vid4/Alexander.pdf URL http://www.aei.mpg.de/~pau/conf_vid4/Alexander.pdf
- [16] Gillessen S, Eisenhauer F, Trippe S, Alexander T, Genzel R, Martins F and Ott T 2009 *ApJ* **692** 1075–1109
- [17] Gould A and Quillen A C 2003 *ApJ* **592** 935–940
- [18] Perets H B, Hopman C and Alexander T 2007 *ApJ* **656** 709–720
- [19] Hills J G 1988 *Nature* **331** 687–689
- [20] Levin Y 2007 *MNRAS* **374** 515–524 (*Preprint* astro-ph/0603583)
- [21] Do T, Ghez A M, Morris M R, Lu J R, Matthews K, Yelda S and Larkin J 2009 *ApJ* **703** 1323–1337
- [22] Buchholz R M, Schödel R and Eckart A 2009 *A&A* **499** 483–501
- [23] Bartko H *et al.* 2010 *ApJ* **708** 834–840
- [24] Gallego-Cano E, Schödel R, Dong H, Nogueras-Lara F, Gallego-Calvente A T, Amaro-Seoane P and Baumgardt H 2017 *ArXiv e-prints* (*Preprint* 1701.03816)
- [25] Schödel R, Gallego-Cano E, Dong H, Nogueras-Lara F, Gallego-Calvente A T, Amaro-Seoane P and Baumgardt H 2017 *ArXiv e-prints* (*Preprint* 1701.03817)
- [26] Bartko H *et al.* 2009 *ApJ* **697** 1741–1763